Journal of Applied Polymer Science

Preparation and Characterization of Poly(ε-caprolactone-*co*-*p*-dioxanone)-poly(ethylene glycol)-Poly(ε-caprolactone-*co*-*p*-dioxanone)/Bioactive Inorganic Particle Nanocomposites

Rui Chen, Jianyuan Hao
State Key Lab of Electronic Films and Integrated Devices, School of Microelectronics and Solid State Electronics, University of Electronic Science and Technology of China, Chengdu, Sichuan 610054, People's Republic of China
Correspondence to: J. Hao (E-mail: jyhao@uestc.edu.cn)

ABSTRACT: With an aim to develop injectable hydrogel with improved solution stability and enhanced bone repair function, thermogelling poly(ε-caprolactone-*co*-*p*-dioxanone)-poly(ethylene glycol)-poly(ε-caprolactone–*co*-*p*-dioxanone) (PECP)/bioactive inorganic particle nanocomposites were successfully prepared by blending the triblock copolymer (PECP) with nano-hydroxyapatite (*n*-HA) or nano-calcium carbonate (*n*-$CaCO_3$). The hydrogel nanocomposites underwent clear sol–gel transitions with increasing temperature from 0 to 50°C. The obtained hydrogel nanocomposites were investigated by ^{1}H NMR, FT-IR, TEM, and DSC. It was found that the incorporation of inorganic nanoparticles into PECP matrix would lead to the critical gelation temperature (CGT) shifting to lower values compared with the pure PECP hydrogel. The CGT of the hydrogel nanocomposites could be effectively controlled by adjusting PECP concentration or the content of inorganic nanoparticles. The SEM results showed that the interconnected porous structures of hydrogel nanocomposites were potentially useful as injectable scaffolds. In addition, due to the relatively low crystallinity of PECP triblock copolymer, the aqueous solutions of the nanocomposites could be stored at low temperature (5°C) without crystallization for several days, which would facilitate the practical applications. The PECP/bioactive inorganic particle hydrogel nanocomposites are expected to be promising injectable tissue engineering materials for bone repair applications. © 2013 Wiley Periodicals, Inc. J. Appl. Polym. Sci. 129: 2287–2293, 2013

KEYWORDS: nanoparticles; nanowires and nanocrystals; composites; biodegradable

Received 20 September 2012; accepted 13 December 2012; published online 17 January 2013
DOI: 10.1002/app.38948

INTRODUCTION

Thermosensitive hydrogels are promising injectable materials for a wide variety of pharmaceutical and biomedical applications. The three-dimensional polymeric networks of the hydrogels were suitable for drug controlled release system[1–4] and tissue engineering.[5–8] Besides their great biocompatibility, thermogelling hydrogels have the advantages including ease of applications, localized delivery for a site-specific action, prolonged delivery periods and improved patient compliance. In recent years, a great variety of physically crosslinked amphiphilic hydrogels that consist of biodegradable hydrophilic and hydrophobic blocks have been reported in the opening literature, such as poly(glycolic acid)/poly(ethylene glycol) (PGA/PEG),[9] poly(ε-caprolactone)/poly(ethylene glycol) (PCL/PEG),[10,11] poly (lactide)/poly(ethylene glycol) (PLA/PEG),[12] poly(lactic acid-co-glycolic acid)/poly(ethylene glycol) (PLGA/PEG).[13,14] Among the hydrogels mentioned above, PCL/PEG hydrogels have been extensively studied and developed in the reported articles. However, the high tendency of crystallization for PCL block results in the instability of the copolymer solution state, which undermining the practical handling property. To solve this problem, other degradable units were introduced into the PCL block to hinder the crystallization of the copolymer by disruption of chain regularity and to improve the copolymer solution stability.[15,16]

In the past decade, biopolymers/inorganic particle composites have attracted more and more attention for their bioactivity, improved interfacial bonding, and reinforced mechanical properties[17–19] and have been widely applied in the fields of bone-repairing devices, bone substitute materials, and bone tissue engineering.[20–22] The inorganic particles, such as hydroxyapatite (HA),[23] calcium carbonate ($CaCO_3$),[24] beta-tricalcium phosphates (β-TCP),[25] calcium sulphate dihydrate (CSD) etc. are of great interest for the development of composite biomaterials which are suitable for cell's attachment and proliferation. Thus, the blending of biodegradable thermosensitive hydrogels with

bioactive inorganic nanoparticle is expected to combine the advantages of both components in a body and give rise to novel injectable tissue engineering scaffolds with bone repair activity.[26]

In this work, we produced novel biodegradable injectable materials by blending thermogelling poly(ε-caprolactone-co-p-dioxanone)-poly(ethylene glycol)-poly(ε-caprolactone-co-p-dioxanone) (PECP) copolymer with nano-hydroxyapatite (*n*-HA) or nano-calcium carbonate (*n*-$CaCO_3$) under ultrasonic condition. The incorporation of p-dioxanone (PDO) units into the hydrophobic block of the copolymer was used to decrease the crystallizability of PCL segments and improve the stability of the composite aqueous solutions. The adding of *n*-HA or *n*-$CaCO_3$ particles into the hydrogel was expected to endow the materials with good osteoconductivity. In this article, the sol–gel transitions, structures, crystallinity, solution stability for the hydrogel nanocomposites were mainly investigated and discussed.

EXPERIMENTAL

Materials

PEG1500 was purchased from Chengdu Kelong Chemical Corporation (Chengdu, China). ε-Caprolactone (CL) was purchased from Acros and distilled over calcium hydride under reduced pressure prior to polymerization. PDO was prepared in our laboratory according to a published procedure,[27] and recrystallized from ethyl acetate before use. Stannous2-ethylhexanoate was purchased from Sigma and used without any further purification. The *n*-$CaCO_3$ powder (diameter < 1 μm) was provided by Shenyang Dongda Fulong Industrial Minerals R&D Co. (Shenyang, China) and used as received. The *n*-HA power (diameter < 1 μm) was prepared in our laboratory according to the literature.[28]

Synthesis of PECP Triblock Copolymer

The PECP triblock copolymer was prepared by ring-opening polymerization of CL and PDO in the presence of PEG as a macromolecular initiator and stannous octoate as a catalyst. A typical synthesis procedure is shown below. Three grams of PEG ($M_w = 1500$) and appropriate amounts of CL/PDO comonomers at a certain feed ratio were introduced into a dry flask at room temperature under nitrogen. The flask was then degassed under vacuum and replaced with nitrogen for several times with 30 min as an interval to remove the residual water and oxygen in the reaction system. Then, stannous octoate was added to the reaction mixtures and stirred at 150°C for 12 h. The crude product was precipitated into diethyl ether. The resultant polymer was purified by redissolution into methylene chloride and precipitation from diethyl ether for at least there times. The residual solvent was removed under vacuum at 80°C overnight. The final yield was about 83%.

Preparation of PECP/Inorganic Particle Hydrogel Nanocomposites

Two grams of PECP triblock copolymer and appropriate amount of deionized water were mixed together, and then the tube containing the mixture was incubated in an air incubator at 0°C and shaken at 60 rpm over a period of time until a completely transparent solution was obtained. Afterward appropriate amount of inorganic particle was added to the fresh prepared PECP solution, and the PECP/inorganic particle hydrogel nanocomposite was thus obtained after the mixture was further incubated in a water bath for 30 min under ultrasonication.

The percentage of inorganic particle contained in the nanocomposites was expressed as the mass ratio of inorganic particle weight to the total mass of solid state (PECP triblock copolymer and inorganic particle without water). The PECP concentration of the hydrogel was expressed as the mass ratio of PECP triblock copolymer weight to the total mass of PECP triblock copolymer and deionized water.

Proton Nuclear Magnetic Resonance (^{1}H NMR)

A NMR spectrometer (Bruker ARX-300) was used for ^{1}H NMR (in $CDCl_3$) measurement to investigate the composition of the triblock copolymer in the presence of TMS as an internal standard.

Fourier Transform Infrared Resonance (FT-IR)

FTIR spectra of the nanocomposites were recorded using a Nicolet 200SXV FTIR (USA) spectrometer with a wavenumber resolution of 2 cm^{-1}. The samples were mixed with KBr and then pressed into pellets. The spectra were recorded between 4000 and 450 cm^{-1}.

Transmission Electron Microscopy (TEM)

TEM was used to observe the images of inorganic particles dispersed in the PECP aqueous solution. The well mixed PECP/inorganic particles aqueous solution by ultra-sonification was diluted by pure PECP aqueous solution and then mounted on 400 mesh copper grids. The obtained sample was examined by a Phillips CM200 TEM with a LaB6 filament operating at 100 kV.

Scanning Electron Microscopy (SEM)

The surface morphologies of the freeze-dried PECP hydrogel and PECP/inorganic particle hydrogel nanocomposite were examined using a JEOL scanning electron microscope (model JSM-6300) after coating the samples with a thin layer of gold by vacuum deposition. The samples were prepared by freeze-drying in a vacuum for 72 h before the test.

Sol–Gel Transition

The sol–gel transition was determined by the test tube inverting method with a temperature increment of 1°C per step.[29] The vials with a diameter of 1.1 cm containing a serial given concentrations of copolymer solutions from 15 wt % to 30 wt % and different contents of inorganic particles were immersed in a water bath at a designated temperature for 20 min. A gel state was determined by visual observation that no macroscopic phase flowing occurred when inverting the tube for 1 min.

Differential Scanning Calorimetry (DSC)

The thermal properties of the synthesized copolymer and frozen dried nanocomposites were investigated by TA DSC Q20 instrument in aluminum pans under nitrogen. The samples were first heated to 80°C and held for 5 min to erase the thermal history. The cooling curves were recorded when the samples were cooled from 80°C to −60°C at a nominal rate of 10°C/min. After keeping the samples at −60°C for 5 min, the heating curves

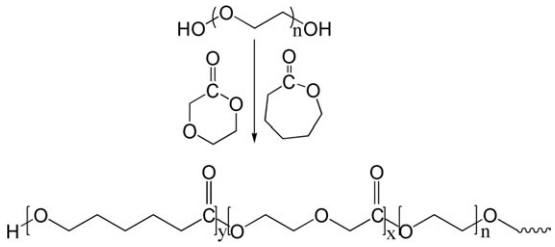

Figure 1. Synthetic scheme of P(CL–PDO)–PEG–P(CL–PDO) copolymer.

were recorded when they were subsequently heated again to 80°C at a nominal rate of 10°C/min.

Degradation *in vitro*

The solutions of pure PECP copolymer and the nanocomposites (25 wt %) were prepared in phosphate buffer saline (PBS pH 7.4). Each solution (2.0 mL) was injected into a preheated 10 mL test tube with a diameter of 1.1 cm at 37°C for 5 min to form a gel. Eight milliliters of phosphate buffer was added to the formed gel and shaken at 60 rpm. The samples were incubated in a water bath at 37°C and taken at designated time intervals, supernatant was removed, and the remaining samples were freeze-dried for 24 h. The degree of degradation was determined by measuring the molecular weight change of the residual polymer on waters 2414/1515 gel permeation chromatography (GPC) using polystyrene as standards and tetrahydrofuran as solvent.

RESULTS AND DISCUSSION

Synthesis and Characterization of the PECP Triblock Copolymer

The PECP triblock copolymer was synthesized by ring-opening polymerization of PDO and CL monomers on to the PEG in the presence of stannous octoate as a catalyst (Figure 1). The resulted copolymer was characterized by ^{1}H NMR (Figure 2). The characteristic peaks at around 4.33 ppm (2H, *t*) (a), 4.18 ppm (2H, *s*) (c), 3.78 ppm (2H, *t*) (b) are assigned to the methylene protons of the PDO units and the chemical shifts at around 2.3 ppm (2H, *t*), 4.1 ppm (2H, *t*) are assigned to the α,ω-methylene protons of CL units, respectively. The chemical composition and molecular weight (M_n) of the PECP copolymer could be calculated from the ^{1}H NMR results. The PECP triblock copolymer synthesized in this article was expressed as (CL/PDO) $_{14.2/1.6}$-(EG)$_{34.1}$-(CL/PDO)$_{14.2/1.6}$ (CL, PDO and EG represent the repeat units of PCL, PPDO and PEG, respectively). The M_n (NMR) value was calculated as 5080 Dalton, considering the molecular weight of PEG is 1500 and the formation of well-defined triblock copolymer.

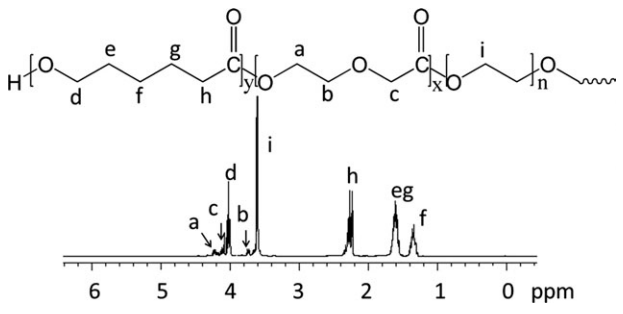

Figure 2. ^{1}H NMR spectrum of P(CL–PDO)–PEG–P(CL–PDO) copolymer.

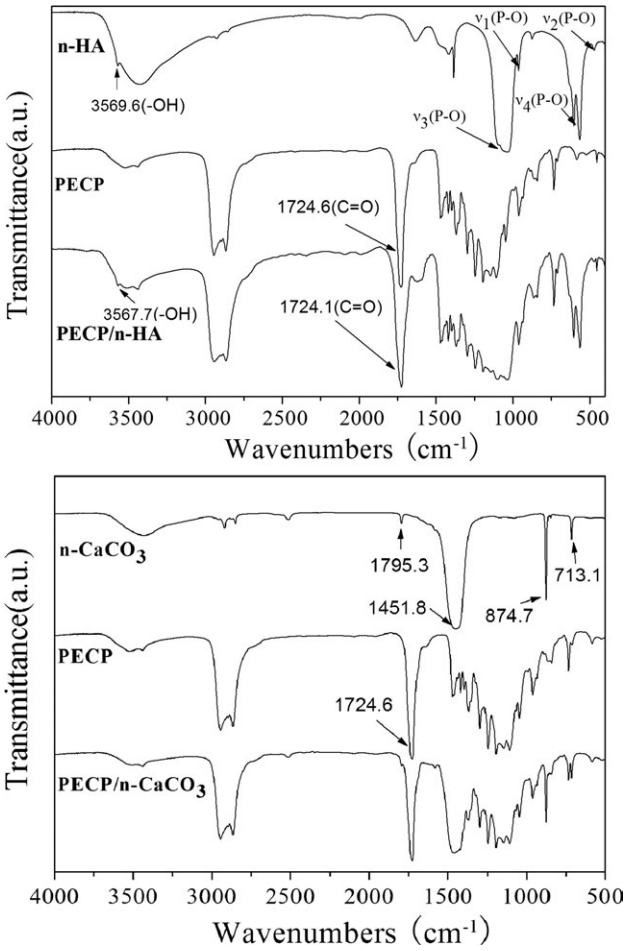

Figure 3. FT-IR spectra for PECP/*n*-HA nanocomposite (upper) and PECP/*n*-$CaCO_3$ nanocomposite (lower).

Characterization of the PECP/Inorganic Particle Hydrogel Nanocomposites

Figure 3 presents the FT-IR spectra of the PECP/ inorganic particle nanocomposites. In Figure 3 (upper), the main characteristic peaks positioned at 1,095, 1,045, 955, 610, and 570 cm^{-1} are due to PO_4^{-3} groups for pure *n*-HA component, corresponding to P—O asymmetrical and symmetrical stretching vibrations and O—P—O bending vibration. These characteristic peaks were also clearly observed for the PECP/*n*-HA nanocomposite, indicating the presence of *n*-HA particles in the hydrogel structure. In Figure 3 (lower), the main characteristic peaks for pure *n*-$CaCO_3$ and PECP components, still appeared with identical positions in the FT-IR spectrum of the PECP/*n*-$CaCO_3$ nanocomposite. It could be concluded that the PECP/ inorganic particle nanocomposites were just the physical mixtures.

The TEM photographs of the PECP/inorganic particle nanocomposites in aqueous solutions were shown in Figure 4. The PECP concentration in aqueous solutions was 20 wt % and the

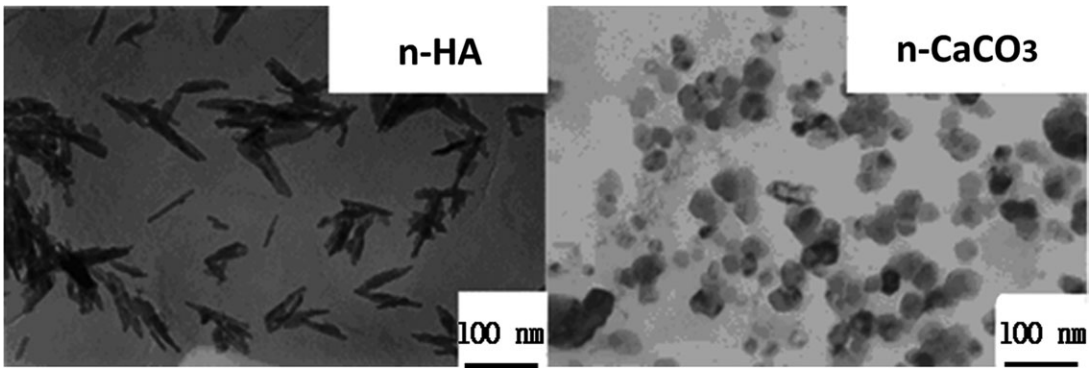

Figure 4. TEM images of *n*-HA nanoparticles (left) and *n*-$CaCO_3$ nanoparticles (right) dispersed in the PECP aqueous solution.

content of inorganic particles in the nanocomposites was 20 wt %. To observe the dispersion of inorganic particles in the PECP aqueous solution, the content of inorganic particles in the nanocomposites was reduced from 20 wt % to 0.1 wt % by dilution with pure 20 wt % PECP aqueous solution. As can be seen in the images, the *n*-HA and *n*-$CaCO_3$ particles have a good dispersion with nano-scale in the PECP aqueous solution.

The microstructures of the freeze-dried hydrogel and nanocomposite samples were examined using SEM (Figure 5), revealing the homogenous porous structures. The introduction of inorganic particles did not change the main interconnected porous morphology of the PECP hydrogel. The included *n*-HA and *n*-$CaCO_3$ particles showed good dispersion within the PECP matrix, with average size of particle clusters smaller than 1 μm and distinct boundaries observed. The pore sizes of all the three samples were in the range of 10 μm to 25 μm, which were suitable for cell growth, allowing the nutrient and waste diffusion.[30]

Phase Transition Behavior of PECP/ Inorganic Particle Hydrogel Nanocomposites

The phase transition behavior of pure PECP hydrogel and the nanocomposites at different temperatures are clearly presented in Figure 6. Due to the hydration of PEG block, the PECP triblock copolymer could dissolve into water to form the flowable solution at room temperature (25°C), in which micelles with a shell–core structure were formed. Under this circumstance, the solution was injectable because of low viscosity. When the solution was heated, the micelles aggregated to form micellar groups, leading to the formation of steady gel around the physiological temperature (37°C). While the temperature was further increased, the gel changed into a turbid solution due to the strong dehydration effect of PEG block and the copolymer precipitated out from the solution. As is shown in Figure 6, similar to pure PECP hydrogel, the PECP/inorganic particle hydrogel nanocomposites also displayed solution gel transition behavior that responded to the environmental temperature like that of pure PECP hydrogel.

The effect of introducing inorganic particles on the phase transition behavior of the PECP hydrogel is presented in Figures 7 and 8. The inorganic particles enhanced the interactions between the hydrophobic domains of micelles in the hydrogel nanocomposites, due to the interfacial Van der Waals force between the particles and the copolymer molecules. Thus, the critical gelation temperatures (CGT) of PECP/*n*-HA and PECP/*n*-$CaCO_3$ hydrogel nanocomposites were lower than that of pure PECP hydrogel, and the temperatures for gel to become turbid solution were shifted to higher values. With increasing the content of inorganic particles, the sol–gel transition behavior of PECP/inorganic particle hydrogel nanocomposites changed more significantly. As can be seen in Figure 9, the gel

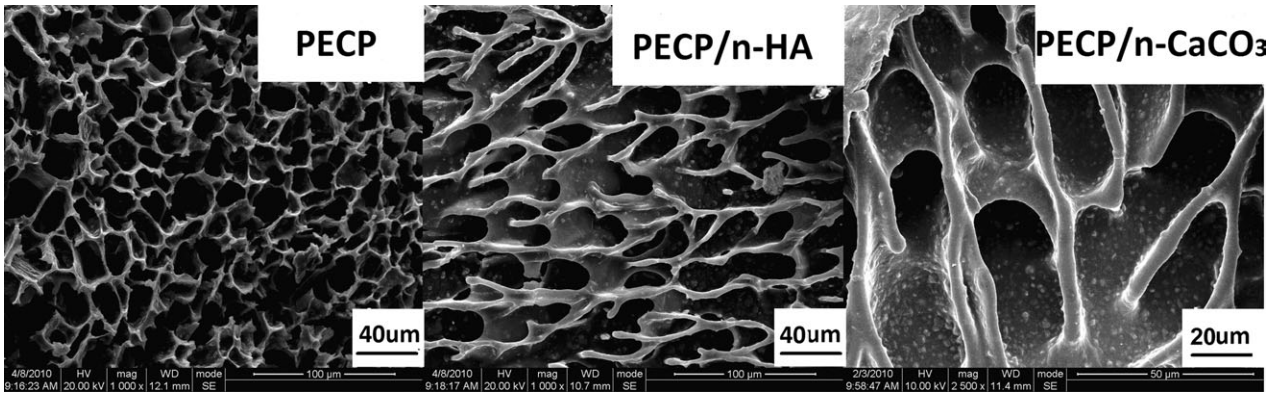

Figure 5. SEM images of freeze-dried pure PECP hydrogel (left), PECP/*n*-HA hydrogel nanocomposite containing 20 wt % *n*-HA (middle) and PECP/*n*-$CaCO_3$ hydrogel nanocomposite containing 20 wt % *n*-$CaCO_3$ (right). The PECP concentration in aqueous solutions for pure hydrogel and the nanocomposites was fixed at 25 wt %.

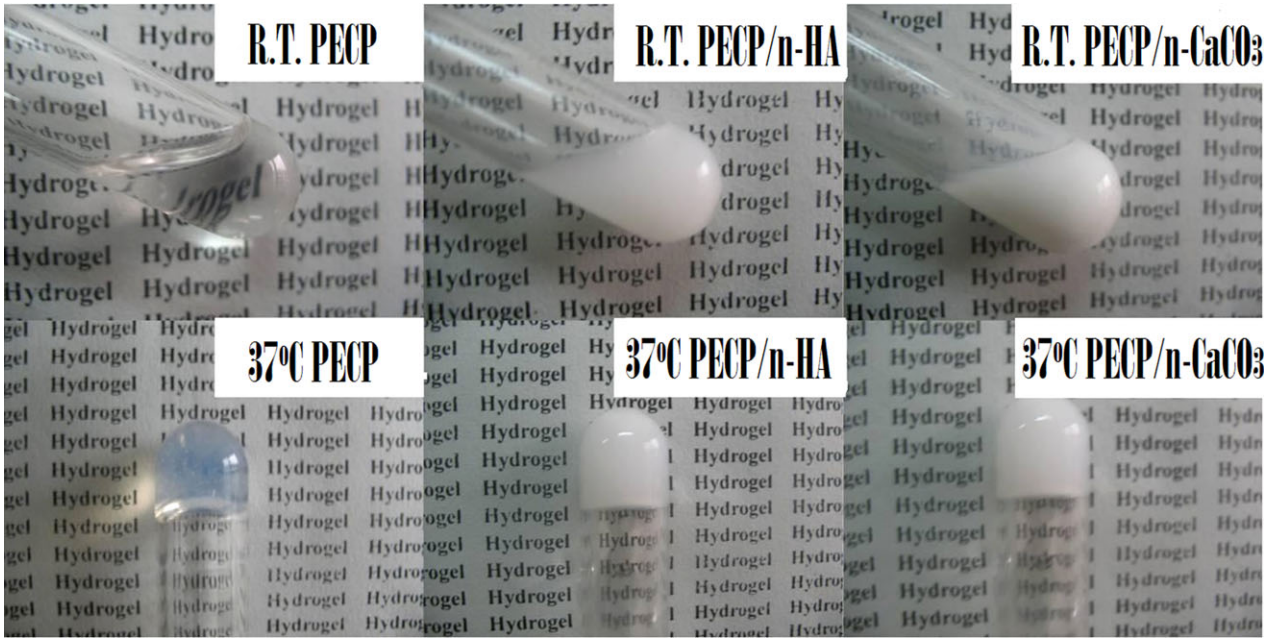

Figure 6. The pictures of thermosensitive phase transition of pure PECP hydrogel, PECP/*n*-HA hydrogel nanocomposite containing 20 wt % *n*-HA and PECP/*n*-$CaCO_3$ hydrogel nanocomposite containing 20 wt % *n*-$CaCO_3$ at the same PECP concentration (25 wt %). [Color figure can be viewed in the online issue, which is available at wileyonlinelibrary.com.]

phase window of PECP/*n*-HA was widened than *n*-$CaCO_3$/PECP under the same loading of inorganic particles, which might be attributed to the stronger physical interaction between *n*-HA particles and PECP molecules.

Thermal Behavior

DSC thermograms of PECP triblock copolymer and PECP/inorganic particle nanocomposites are presented in Figure 10. In the cooling curves, all the samples displayed a lower peak from −20 to 0°C and a higher peak from 0 to 20°C, which were assigned to the crystalline regions of PEG and PCL segments, respectively. The two endothermic peaks ranging at 20–50°C in the heating curves came from the melting of crystallized and recrystallized PCL segments. The peak temperatures for PCL crystallization of PECP/inorganic particle nanocomposites were obviously higher than that for pure PECP, which suggested that the well dispersed inorganic particles in the hydrogel nanocomposites acted as the center of nucleation and induced the earlier formation of PCL nuclei. Compared with PECP/*n*-HA, the higher crystallization temperature of PECP/*n*-$CaCO_3$ nanocomposite was probably related to the increase in the density of active nuclei, which indicated that *n*-$CaCO_3$ was a better nucleating agent than *n*-HA for PCL segments.

The melting peaks of PECP/inorganic particle nanocomposites during the heating cycle shifted to a higher temperature region

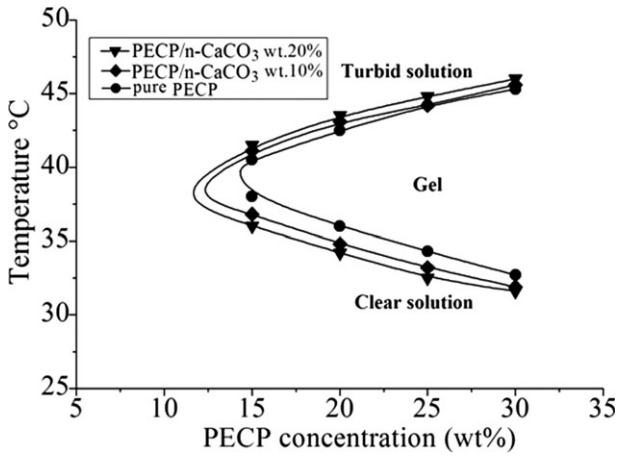

Figure 7. Phase transition curves of pure PECP hydrogel and PECP/*n*-$CaCO_3$ hydrogel nanocomposite containing 10 or 20 wt % $CaCO_3$ at different PECP concentrations.

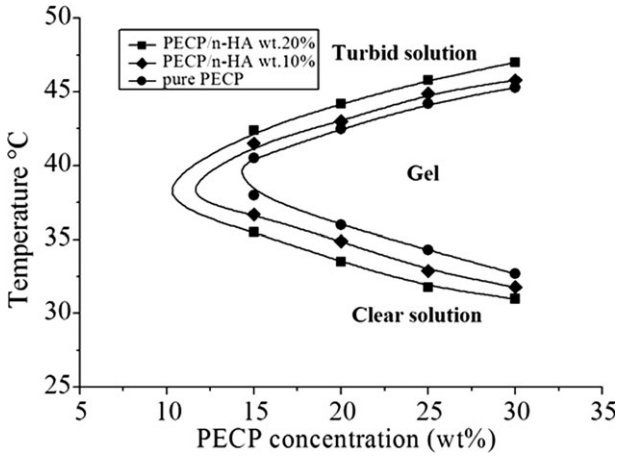

Figure 8. Phase transition curves of pure PECP hydrogel and PECP/*n*-HA hydrogel nanocomposites containing 10 or 20 wt % *n*-HA at different PECP concentrations.

Applied Polymer SCIENCE

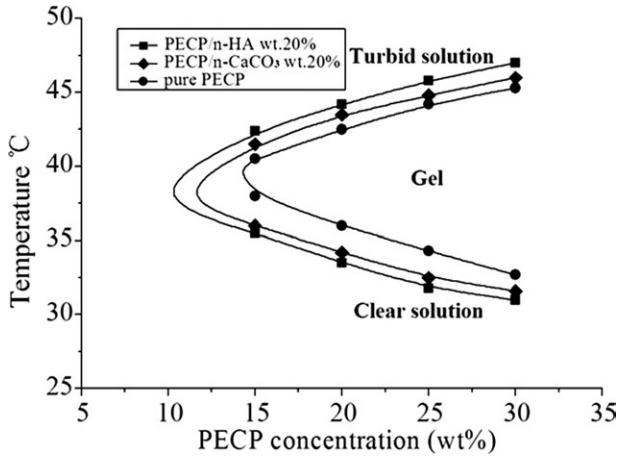

Figure 9. Comparison of phase transition curves of pure PECP hydrogel, PECP/*n*-HA hydrogel nanocomposites containing 20 wt % *n*-HA and PECP/*n*-$CaCO_3$ hydrogel nanocomposite containing 20 wt % *n*-$CaCO_3$.

as compared with pure PECP copolymer. This might be due to the presence interfacial interaction between the PECP matrix and inorganic particles, leading to partial immobilization of the PCL segments. The degree of crystallinity of the CL units for pure PECP copolymer and the nanocomposites can be calculated according to the following relation:

$$X_C = \Delta H_f / (w \times \Delta H_{f,100\%})$$

where $\Delta H_{f,100\%}$ and ΔH_f indicate the heats of fusion for a 100% crystalline CL homopolymer and the copolymer, respectively, w is the weight fraction of CL units in the copolymer. To calculate X_c, the literature value of $\Delta H_{f,100\%} = 142$ J/g was used and the values was 53% (PECP), 56% (PECP/*n*-HA 10 wt %), 58% (PECP/*n*-HA 20 wt %) and 59% (PECP/*n*-$CaCO_3$ 20 wt %), respectively. Similar to the trend that exhibited by the melting or crystallization temperature, the crystallinity of the copolymer in the nanocomposites are slightly higher than that for pure PECP, further indicating the effect of inorganic particles as nucleation agents.

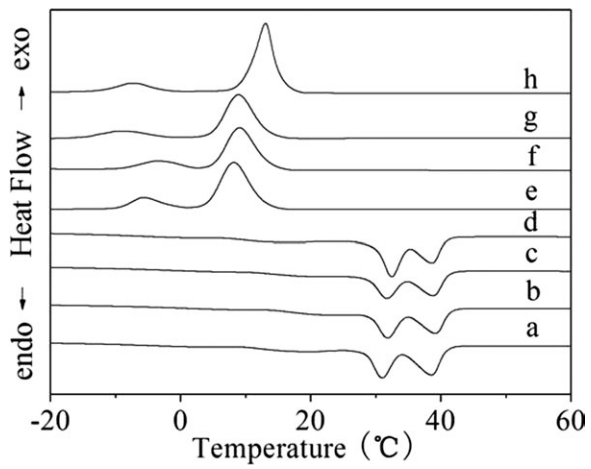

Figure 10. DSC curves of pure PECP triblock copolymer and PECP/inorganic particle nanocomposites. a, b, c, and d are heating curves and e, f, g, and h are cooling curves for pure PECP, PECP/*n*-HA nanocomposite with 10 wt % *n*-HA, PECP/*n*-HA nanocomposite with 20 wt % *n*-HA and PECP/*n*-$CaCO_3$ nanocomposite with 20 wt % *n*-$CaCO_3$, respectively.

Aqueous Solution Stability

The PCL–PEG–PCL and PEG–PCL–PEG hydrogels are well developed thermosensitive injectable biomaterials. However, because of the high crystallizability of pure PCL segments and their high crystallization temperature over 20°C, the aqueous solutions of above mentioned two copolymers would easily turn into opaque gels within 20 min at room temperature.[31] To improve the stability of the copolymer aqueous solution at low temperature, we incorporated PDO units into the copolymer to decrease the crystallizability of PCL segments. The hindrance of crystallization was clearly exhibited by the much decreased crystallization temperature of the copolymer below 10°C (Figure 10). As a result, the thermogelling PECP aqueous solution prepared in this article could be stored in refrigerator (5°C) for several days without crystallization occurred. Although the addition of inorganic nanoparticles would accelerate the nucleation process of the copolymer, the aqueous solutions of PECP/inorganic particle nanocomposites still kept their flowability as injectable liquid for more than 2 days, which would facilitate the practical applications.

Degradation of PECP/Inorganic Particle Hydrogel Nanocomposites

The *in vitro* degradation behaviors of pure PECP hydrogel and PECP/inorganic particle nanocomposites were examined over a 24-week period by GPC and the results are presented in Figure 11. For pure PECP hydrogel, the volume of the hydrogel did not change much with degradation time. However, the molecular weight of the copolymer decreased gradually, with the hydrogel state changing from semi-transparent to opaque. After 20 weeks, the boundary between the buffer and the gel disappeared and a viscous degraded liquid formed. The PECP/inorganic particle nanocomposites showed similar degradation behaviors as that for pure PECP hydrogel, but with retarded times about 2 (PECP/*n*-CaCO3) or 4 (PECP/*n*-HA) weeks later

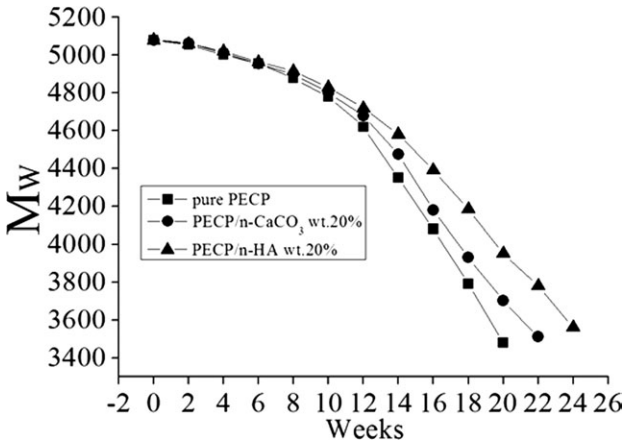

Figure 11. The degradation behaviors of pure PECP hydrogel, PECP/*n*-HA nanocomposite with 20 wt % *n*-HA and PECP/*n*-$CaCO_3$ nanocomposite with 20 wt % *n*-$CaCO_3$ under pH 7.4, 37°C.

for the gel to turn into viscous liquid. This fact indicates that the addition of inorganic particles could retard the degradation of the copolymer, which was also exhibited by the change of molecular weight of the copolymer. It was presumed that the base/acid neutralization reaction between the degraded products and the inorganic particles accounted for the retarded degradation behaviors of the hydrogel nanocomposites.

CONCLUSIONS

Serial thermogelling aqueous solutions based on PECP/*n*-HA and PECP/*n*-$CaCO_3$ nanocomposites undergoing sol–gel transitions were successfully prepared. The phase transition behaviors of the obtained nanocomposite aqueous solutions could be effectively adjusted by varying the content of inorganic particles. The inorganic particles distributed uniformly and finely within the hydrogel matrix and did not disrupt the 3D interconnected pore structure. The aqueous solution stability of the obtained nanocomposites was well at low temperature due to the decreased crystallizability of the PCL segments by the incorporation of PDO units. These novel biodegradable hydrogel nanocomposites are promising injectable materials for bone tissue engineering applications.

ACKNOWLEDGMENTS

This work was supported by the National Natural Sciences Fund of China (No. 30970725, No. 51273034), the Opening Project of the State Key Laboratory of Polymer Materials Engineering (Sichuan University, KF201201).

REFERENCES

1. Gong, C. Y.; Shi, S. A.; Dong, P. W.; Yang, B.; Qi, X. R.; Guo, G.; Gu, Y. C.; Zhao, X.; Wei, Y. Q.; Qian, Z.Y. *J. Pharm. Sci.* **2009**, *4684*, 98.
2. Gong, C. Y.; Shi, S.; Wu, L.; Gou, M. L.; Yin, Q. Q.; Guo, Q. F. *Acta Biomater.* **2009**, *3258*, 5.
3. Jiang, Z. Q.; Hao, J. Y.; You, Y. J. *J. Pharm. Sci.* **2009**, *2603*, 98.
4. Xun, W.; Wu, D. Q.; Li, Z. Y.; Wang, H. Y.; Huang, F. W.; Cheng, S. X.; Zhang, X. Z.; Zhuo, R. X. *Macromol. Biosci.* **2009**, *1219*, 9.
5. Park, S. H.; Choi, B. G.; Joo, M. K.; Han, D. K.; Sohn, Y. S.; Jeong, B. *Macromolecules* **2008**, *6486*, 41.
6. Fu, S. Z.; Guo, G.; Gong, C. Y.; Zeng, S.; Liang, H.; Luo, F.; Zhang, X. N.; Zhao, X.; Wei, Y. Q.; Qian, Z. Y. *J. Phys. Chem. B.* **2008**, *16518*, 113.
7. Ekenseair, A. K.; Boere, K. W. M.; Tzouanas, S. N.; Vo, T. N.; Kasper, F. K.; Mikos, A. G. *Biomacromolecules* **2012**, *13*, 9.
8. Wang, L. M.; Stegemann, J. P. *Biomaterials* **2010**, *31*, 14.
9. Bencherif, S. A.; Srinivasan, A.; Sheehan, J. A.; Walker, L. M.; Gayathri, C.; Gil, R.; Hollinger, J. O.; Matyjaszewski, K.; Washburn, N. R. *Acta Biomater*, **2009**, *1872*, 5.
10. Bae, S. J.; Suh, J. M.; Sohn, Y. S.; Bae, Y. H.; Kim, S. W.; Jeong, B. *Macromolecules* **2005**, *5260*, 38.
11. Hwang, M. J.; Suh, J. M.; Bae, Y. H.; Kim, S. W. *Biomacromolecules* **2005**, *885*, 6.
12. Tew, G. N.; Sanabria-DeLong, N.; Agrawal, S. K.; Bhatia, S. R. *Soft Matter* **2005**, *253*, 1.
13. Jeong, B.; Bae, Y. H.; Kim, S. W. *Macromolecules* **1999**, *7064*, 32.
14. Jeong, B.; Bae, Y. H.; Kim, S. W. *J. Control. Release* **2000**, *155*, 63.
15. Jiang, Z. Q.; Deng, X. M.; Hao, J. Y. *J. Polym. Sci. Part A: Polym. Chem.* **2007**, *4091*, 45.
16. Jiang, Z. Q.; You, Y. J.; Deng, X. M.; Hao, J. H. *Polymer* **2007**, *4786*, 48.
17. Shikinami, Y.; Okuno, M. *Biomaterials* **2001**, *3197*, 22.
18. Ural, E.; Kesenci, K.; Fambri, L.; Migliaresi, C.; Piskin, E. *Biomaterials* **2000**, *2137*, 21.
19. Bai, W.; Chen, D. L.; Zhang, Z. P.; Li, Q.; Zhang, D. J.; Xiong, C. D. *J. Biomed. Mater. Res. B.* **2009**, *945*, 1.
20. Wei, G. B.; Ma, P. X. *Biomaterials* **2004**, *4749*, 25.
21. Kobayashi, M.; Nakamuro, T.; Tamura, J.; Kokubo, T.; Kikutani, T. *J. Biomed. Mater. Res.* **2000**, *301*, 37.
22. Wang, M.; Joseph, R.; Bonfield, W. *Biomaterials* **1998**, *2357*, 19.
23. Valago, A. P.; Srro, A. D.; Fernandes, A. C.; Saramago, B. J. V. *J. Biomed. Mater. Res.* **2000**, *345*, 49.
24. Vuola, J.; Goransson, H.; Bohling, T.; Asko-Seljavaara, S. *Biomaterials* **1996**, *1761*, 17.
25. Kikuchi, M.; Suetsugu, Y.; Tanaka, J.; Akao, M. *J. Mater. Sci. Mater. Med.* **1997**, *361*, 8.
26. Moon, H. J.; Ko, D. Y.; Park, M. H.; Joo, M. K.; Jeong, B. *Chem. Soc. Rev.* **2012**, *41*, 14.
27. Wang, H.; Dong, J. H.; Qiu, K. Y.; Gu, Z. W. *Polym. Sin. Acta.* **1997**, *329*, 3.
28. Vuola, J.; Goransson, H.; Bohling, T.; Asko-Seljavaara, S. *Biomaterials* **1996**, *1761*, 17.
29. Alexandrisdis, P.; Holzwarth, J. F.; Hatton, T. A. *Macromolecules* **1994**, *2414*, 27.
30. Fu, S. Z.; Guo, G.; Gong, C. Y.; Zeng, S.; Liang, H.; Luo, F.; Zhang, X. N.; Zhao, X.; Wei, Y. Q.; Qian, Z. Y. *J. Phys. Chem. B* **2009**, *16518*, 113.
31. Park, S. H.; Choi, B. G.; Joo, M. K.; Han, D. K.; Sohn, Y. S.; Jeong, B. *Macromolecules* **2008**, *6486*, 41.